This article has been accepted for publication in a future issue of this journal, but has not been fully edited. Content may change prior to final publication. Citation information: DOI 10.1109/TMAG.2015.2442977, IEEE Transactions on Magnetics

Torque Pulsation Minimization in Spoke-type Interior Permanent Magnet Motors with Skewing and Sinusoidal Permanent Magnet Configurations

Wenliang Zhao[1], Thomas A. Lipo[2], *Life Fellow*, *IEEE*, and Byung-il Kwon[1], *Senior Member*, *IEEE*

[1]Department of Electronic Systems Engineering, Hanyang University, Ansan, 426-791, Korea
[2] Department of Electrical and Computer Engineering, Florida State University, Tallahassee FL, 32306, USA

This paper proposes two approaches to minimize torque pulsations including cogging torque and electromagnetic torque ripple for spoke-type interior permanent magnet (IPM) motors. The first approach is an improved skewing method, in which the rotor-permanent magnets (PMs) are skewed by being symmetrical in the axial direction within one magnet pole pitch for not only reducing torque pulsations but also maintaining maximum available torque and eliminating unbalanced axial electromagnetic forces. The second one is a sinusoidal PM shaping method with the aim of achieving the same advantageous effects as the proposed skewing method. Both of the proposed methods adopt stepped rotor-PM schemes and the effects of the rotor-PM step numbers on motor performance are investigated. To highlight the advantages of the proposed approaches, a spoke-type IPM motor with conventional PM configuration is adopted as the basic model. All the motor characteristics such as back electromotive force (EMF), cogging torque, and electromagnetic torque are predicted by a three-dimensional (3-D) finite element method (FEM) with the aid of JMAG-Designer.

***Index Terms*—Cogging torque, electromotive force (EMF), finite element method (FEM), interior permanent magnet (IPM) motors, sinusoidal PM shape, skewing, spoke-type, torque ripple.**

I. Introduction

INTERIOR permanent magnet (IPM) motors are increasingly popular in various industrial and domestic applications due to the advances in permanent magnet (PM) manufacturing and technology. In particular, the spoke-type IPM motor offers superior performance in terms of relatively high torque (power) density and high efficiency benefiting from the concentrated flux from rotor PMs [1]-[2]. However, the undesirable disadvantages of such motors are the serious distortion of airgap flux density distribution resulting in numerous harmonics in the back EMF, and high torque pulsations including cogging torque and torque ripple [3].

In general, torque pulsations cause unacceptable vibration, acoustic noise, poor position and speed control, performance degradation and even running failures. Accordingly, torque pulsation minimization must be considered when designing for electric motors in practical applications, where design-based or control-based techniques are commonly utilized [4]-[6]. However, the available techniques for spoke-type IPM motors to minimize torque pulsations are very limited and less researched due to their rotor-PM configuration. As one of the most widely used techniques, skewing, which can be either continuous or stepwise, is effective to minimize cogging torque and improve the back-EMF waveform. However, the conventional skewing method is generally employed in surface-mounted PM (SPM) motors and has the disadvantages of reducing the maximum available electromagnetic torque and yielding an unbalanced axial electromagnetic force [7].

Manuscript received March 20, 2015, revised May 13, 2015, accepted June 02, 2015. Corresponding author: Byung-il Kwon (e-mail: bikwon@hanyang.ac.kr).
Digital Object Identifier inserted by IEEE

In this paper, two approaches are proposed to minimize torque pulsations including cogging torque and torque ripple for spoke-type IPM motors. The first approach is designated as an improved skewing method in which the rotor-PMs are skewed by being symmetrical in the axial direction within one magnet pole pitch to reduce torque pulsations, maintain the maximum available torque and to eliminate unbalanced axial electromagnetic forces. The second approach is a sinusoidal PM shaping method with the aim of achieving the same advantageous effects as the proposed skewing method. Both of the proposed methods adopt stepped rotor-PM schemes and the effects of the rotor-PM step numbers on motor performance are investigated. To highlight the advantages of the proposed approaches, a spoke-type IPM motor with conventional rotor-PM configurations is adopted for comparison based on a 3-D FEM by JMAG-Designer.

II. Motor Modeling for the Proposed Approaches

A. Basic Spoke-type IPM Motor

To highlight the advantages of the proposed approaches, a conventional spoke-type IPM motor is adopted as the basic model as shown in Fig. 1. The stator has six slots with concentrated windings as shown in Fig. 1(a). The rotor is inserted with circumferentially magnetized NdFeB magnets in a spoke-type array as shown in Fig. 1(b). The specifications for all the investigated motor models are listed in Table I.

B. Proposed Models with Improved Skewing Method

The cogging torque in PM motors, which is present even without powering the motor, arises from the interaction between the rotor PMs and stator slotted iron structure, which can be predicted by the equation as

$$T_{cogging} = -\frac{\partial W}{\partial \alpha} \tag{1}$$

where W is the stored energy and α is the rotor position.

This article has been accepted for publication in a future issue of this journal, but has not been fully edited. Content may change prior to final publication. Citation information: DOI 10.1109/TMAG.2015.2442977, IEEE Transactions on Magnetics

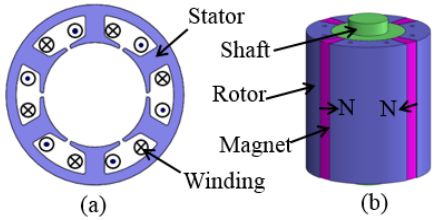

Fig. 1. Basic model. (a) Stator and windings. (b) Rotor with magnets.

TABLE I
SPECIFICATIONS OF THE BASIC MODEL

Item	Unit	Value
Magnet poles/Stator slots	-	4/6
Stator outer diameter	mm	88
Airgap length	mm	0.5
Motor axial length	mm	54
Remanence of magnet	T	0.47

Thus, the total cogging torque can be modeled as the sum of all elementary torques produced by the interaction between the edges of each magnet and stator slot [5]. Then the resultant cogging torque is at a minimum when the skewing angle between two adjacent steps is equal to

$$\theta_{skewing} = \frac{2\pi}{nN_cQ} \tag{2}$$

where n is the number of skewing steps, Q is the number of stator slots, and N_c is the period of cogging torque given by

$$N_c = \frac{2p}{HCF(2p,Q)} \tag{3}$$

where p the number of magnet pole pairs and HCF is a function of the highest common factor.

Fig. 2 shows the skewing models investigated here. The skewing model 1 (M1) is obtained by (3), as shown in Fig. 2(a). To prevent the torque performance from degrading, the skewing model 2 (M2) and model 3 (M3), which are shown in Fig. 2(b) and 2(c) are obtained using (3) and the constraint

$$n\theta_{skewing} + \theta_m \le \theta_p \tag{4}$$

where θ_p is the angular spacing of the magnet pole pitch and θ_m is the angular spacing of two adjacent magnets, which are illustrated in Fig. 2(a) and (c), respectively.

In particular, the proposed skewing model 3 adopts symmetrical rotor-PM configurations in the axial direction to eliminate unbalanced axial electromagnetic forces. It is noted here the PM stacks A_1 and A_2 keep the same magnetized direction in the skewing models 2 and 3 for maintaining the same magnet pole numbers and electric frequency.

C. Proposed Models with Sinusoidal PM Shaping Method

It has been found in [7] that the PM shape in SPM motors substantially affects the back EMF waveform and cogging torque, which can be adopted to minimize torque pulsations in spoke-type IPM motors. The design criteria for the proposed models with a sinusoidal PM shaping method is illustrated in Fig. 3. By means of a unit circle in Fig. 3(a), a sinusoidal rotor shape can be created as shown in the developed view of Fig. 3(b). Taking the middle line of the stack step as a benchmark, the sinusoidal model 1 (M1) is created as shown in Fig. 4(a).

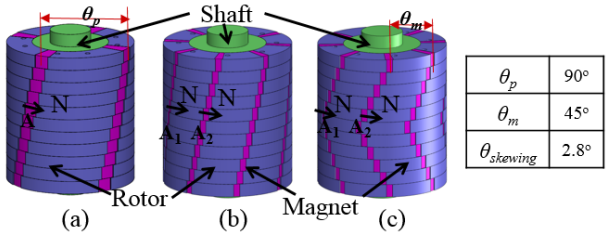

Fig. 2. Proposed models with skewing method. (a) Skewing model 1. (b) Skewing model 2. (c) Skewing model 3 with symmetrical PM configuration.

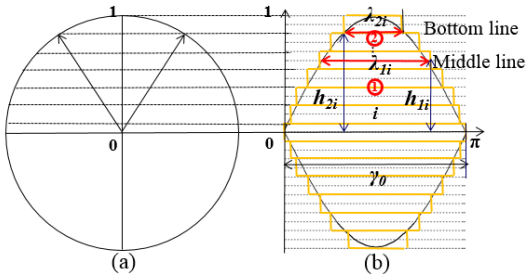

Fig. 3. Design principle of the proposed models with sinusoidal PM shaping method. (a) Unit circle. (b) Developed view of the rotor shape.

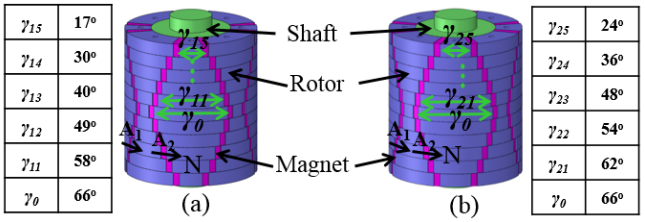

Fig. 4. Proposed models with sinusoidal PM shaping method. (a) Sinusoidal model 1. (b) Sinusoidal model 2.

The height of each step can be expressed as

$$h_{1i} = \frac{2i\text{-}2}{m} \qquad \text{i=1, 2, 3…} \tag{5}$$

where m is the number of stack steps.

The angular width of each step is approximately obtained as

$$\lambda_{1i} = \frac{180 - 2\,arcsin(h_{1i})}{180}\pi \tag{6}$$

Thus, the angular spacing of each step is approximated by

$$\gamma_{1i} = 2\,arcsin(\frac{\lambda_{1i}}{\pi} sin\frac{\gamma_0}{2}) \tag{7}$$

Using the bottom line of the stack step as a benchmark, the sinusoidal model 2 (M2) is created as shown in Fig. 4(b). The height of each step will be

$$h_{2i} = \frac{2i-3}{m} \qquad h_{21}=0;\ \text{i=2, 3…} \tag{8}$$

The angular width of each step is approximately obtained as

$$\lambda_{2i} = \frac{180 - 2\,arcsin(h_{2i})}{180}\pi \tag{9}$$

Thus, the angular spacing of each step is approximated as

$$\gamma_{2i} = 2\,arcsin(\frac{\lambda_{2i}}{\pi} sin\frac{\gamma_0}{2}) \tag{10}$$

The height of the first step in both cases $\lambda_{11}=\lambda_{21}=\pi$ and the mechanical angle of the first step $\gamma_0=66°$ is noted here. The two types of sinusoidal models also adopt symmetrical rotor-PM configurations in the axial direction and the PM stacks A_1 and A_2 keep the same magnetized direction.

This article has been accepted for publication in a future issue of this journal, but has not been fully edited. Content may change prior to final publication. Citation information: DOI 10.1109/TMAG.2015.2442977, IEEE Transactions on Magnetics

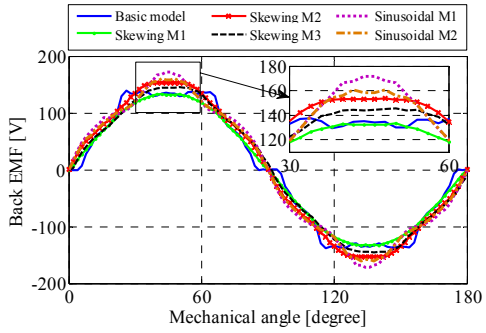

Fig. 5. Comparison of phase back EMFs.

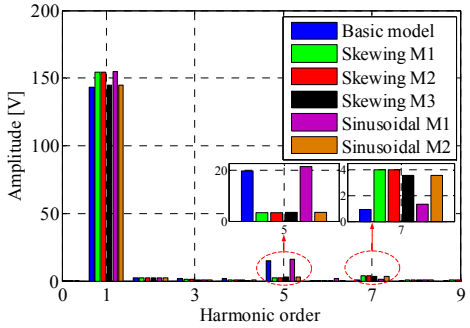

Fig. 6. FFT analysis of phase back EMFs.

III. 3-D FEM Analysis Results

A. Comparison of Motor Characteristics

The 3-D FEM by JMAG-Designer is employed to predict motor characteristics accounting for the axial interactions between the rotor-PM steps. The comparison of phase back EMFs are shown in Fig. 5. Fig. 6 shows the corresponding fast Fourier transform (FFT) analysis. It is found that both of the skewing and sinusoidal models are effective to minimize the harmonics of back EMFs when compared to the basic model. However, the skewing model 1, designed without the skewing constraint, has a lower rms value of back EMF due to the reduction of the useful PM flux linking the stator windings, resulting from the interactions between two adjacent PM poles. The numerical results are listed in Table II.

Fig. 7 shows the comparison of cogging torques. It shows that the skewing models 1 and 2 demonstrate optimal cogging torque minimization but unbalanced axial electromagnetic forces. The unbalanced forces inevitably result in additional vibration and acoustic noise as well as damage to bearing systems as result of their axially asymmetrical structure, as depicted in Fig. 8. The skewing model 3 and sinusoidal model 2 exhibit competitively compromised performance as shown by 62.1% and 69.7% cogging torque suppression, respectively, compared to the basic model, as listed in Table II.

The electromagnetic torques, obtained by feeding the stator windings with sinusoidal current excitations with 3 Arms/mm^2 at 4800 r/min, are compared in Fig. 9. In contrast to the skewing model 1 which has a degradation of average torque, all other proposed models maintain the maximum available torque with highly decreased torque ripple. The torque ripple of the proposed skewing model 3 and sinusoidal model 2 are reduced by 40.0% and 43.2%, respectively, when compared to

TABLE II
FEM Analysis Results of the Investigated Motors

Item	Unit	Basic model	Skewing			Sinusoidal	
			M1	M2	M3	M1	M2
Number of 3-D mesh element	Mill-ion	1.11	1.13	1.14	1.11	1.11	1.14
Back EMF	V	102.6	95.2	109.7	103.3	107.3	107.8
THD of EMF	%	11.84	3.75	3.69	3.75	7.46	7.42
Cogging torque	Nm	0.066	0.006	0.007	0.025	0.026	0.020
Torque	Nm	0.6531	0.6059	0.6857	0.6537	0.6767	0.6753
Torque ripple	%	25.26	9.71	14.29	15.15	15.93	14.36
Power	W	328.28	304.56	344.67	328.58	340.15	339.44
Iron loss	W	22.04	21.35	17.65	16.74	18.04	17.87
Efficiency	%	90.65	90.18	92.12	92.01	91.98	91.96

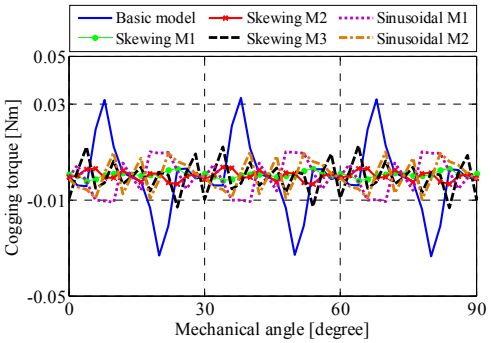

Fig. 7. Comparison of cogging torques.

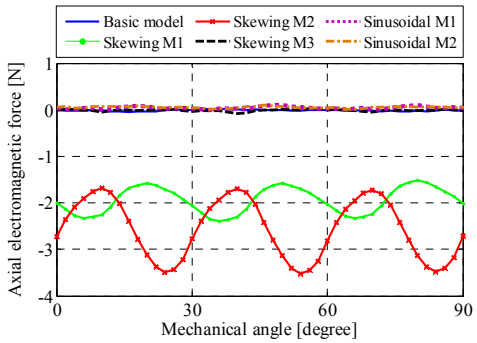

Fig. 8. Comparison of unbalanced axial electromagnetic force.

that of the basic model. Fig. 10 describes the harmonics of electromagnetic torques, which shows that the dominant 6th, 12th, and 18th harmonics are highly suppressed in the proposed models. Furthermore, due to the harmonic minimization in back EMFs and torques, all the proposed models experience lower iron loss which results in higher efficiency compared to the basic model, wherein the efficiency is obtained as in [7].

B. Effects of the Rotor-PM Step Numbers

The effects of the rotor-PM step numbers of the skewing model 3 and sinusoidal model 2 on motor characteristics are explored by 3-D FEM accounting for the axial interactions between the rotor-PM steps. Fig. 11 shows the magnetic flux density distribution. As illustrated in Fig. 11(a), the skewing model 3 with 5 steps exhibits saturation between two adjacent steps in the axial direction, which could lead to severe distortion of the airgap flux density distribution, degradation of output torque and aggravation of torque pulsations [8].

This article has been accepted for publication in a future issue of this journal, but has not been fully edited. Content may change prior to final publication. Citation information: DOI 10.1109/TMAG.2015.2442977, IEEE Transactions on Magnetics

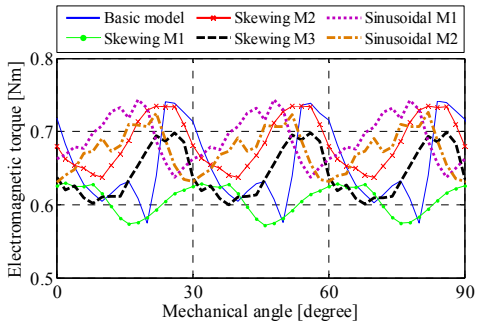

Fig. 9. Comparison of electromagnetic torques.

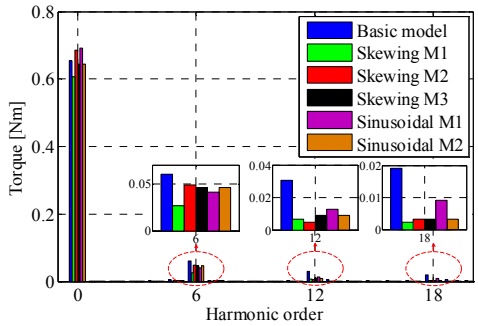

Fig. 10. Comparison of harmonics in electromagnetic torques.

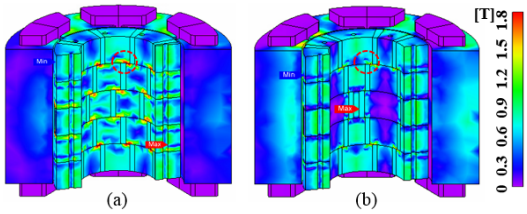

Fig. 11. Magnetic flux density distribution. (a) Skewing model 3 with 5 steps. (b) Sinusoidal model 2 with 5 steps.

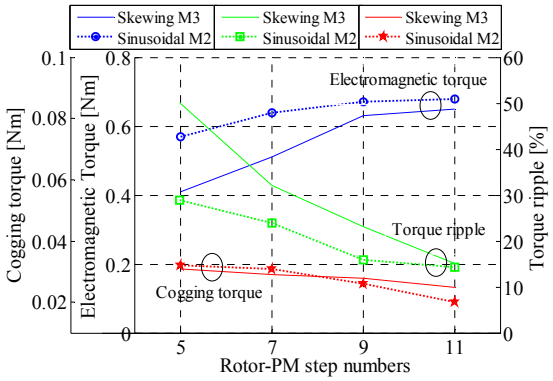

Fig. 12. The effects of the rotor-PM step numbers on motor characteristics.

A similar condition occurs in the sinusoidal model 2 with 5 steps as shown in Fig. 11(b). Fig. 12 shows the relationships of cogging torque, electromagnetic torque, and torque ripple with respect to the rotor-PM step numbers for the skewing model 3 and sinusoidal model 2. The numerical results are listed in Table III. It shows that both models have aggravated cogging torque and torque ripple with highly reduced average torque in fewer steps, which indicates the axial space between two steps should be eliminated by selecting the proper rotor-PM step numbers to prevent magnetic saturation.

TABLE III
THE EFFECTS OF THE ROTOR-PM STEP NUMBERS

Item	Unit	Skewing M3				Sinusoidal M2			
Step numbers	-	5	7	9	11	5	7	9	11
Cogging torque	Nm	0.031	0.029	0.028	0.025	0.032	0.031	0.026	0.020
Torque	Nm	0.41	0.51	0.63	0.65	0.57	0.64	0.67	0.68
Torque ripple	%	50.1	32.1	23.1	15.2	28.9	24.0	15.9	14.4

IV. CONCLUSION

This paper has proposed two approaches, the improved skewing and sinusoidal PM shaping methods, to improve the performance in spoke-type IPM motors. Based on the 3-D FEM analysis by comparing to the basic model, both of the approaches are effective to not only reduce torque pulsations including cogging torque (reduced by above 60%) and torque ripple (reduced by above 40%), but also to maintain the maximum available torque and eliminate unbalanced axial electromagnetic forces. Through an investigation of the effects of the rotor-PM step numbers, it was found that the rotor-PM step numbers in the proposed models should be carefully selected to prevent the magnetic saturation resulting from the axial interactions for high performance in applications.

ACKNOWLEDGMENT

This research was jointly supported by the BK21PLUS program through the National Research Foundation of Korea funded by the Ministry of Education, and the Human Resources Program in Energy Technology of the Korea Institute of Energy Technology Evaluation and Planning (KETEP), granted financial resource from the Ministry of Trade, Industry and Energy, Republic of Korea (20154030200730).

REFERENCES

[1] D. G. Dorrell, M. F. Hsieh, and A. M. Knight, "Alternative rotor designs for high performance brushless permanent magnet machines for hybrid electric vehicles," *IEEE Trans. Magn.*, vol. 48, no. 2, pp. 835-838, Feb. 2012.

[2] M. M. Rahman, K. Kim, and J. Hur, "Design and optimization of neodymium-free SPOKE-type motor with segmented wing-shaped PM," *IEEE Trans. Magn.*, vol. 50, no. 2, p. 7021404, Feb. 2014.

[3] K. Y. Hwang, J. H. Jo, and B. I. Kwon, "A study on optimal pole design of spoke-type IPMSM with concentrated winding for reducing the torque ripple by experiment design method," *IEEE Trans. Magn.*, vol. 45, no. 10, pp. 4712-4715, Oct. 2009.

[4] K. C. Kim, "A novel method for minimization of cogging torque and torque ripple for interior permanent magnet synchronous motor," *IEEE Trans. Magn.*, vol. 50, no. 2, p. 7019604, Feb. 2014.

[5] C. Bianchini, F. Immovilli, E. Lorenzani, A. Bellini, and M. Davoli, "Review of design solutions for internal permanent magnet machines cogging torque reduction," *IEEE Trans. Magn.*, vol. 48, no. 10, pp 2685-2693, Oct. 2012.

[6] Z. Q. Zhu, Y. Liu, and D. Howe, "Minimizing the influence of cogging torque on vibration of PM brushless machines by direct torque control," *IEEE Trans. Magn.*, vol. 42, no. 10, pp. 3512-3514, Oct. 2006.

[7] W. L. Zhao, T. A. Lipo and B. I. Kwon, "Material-efficient permanent-magnet shape for torque pulsation minimization in SPM motors for automotive applications," *IEEE Trans. Ind. Electron.*, vol. 61, no. 10, pp. 5779-5787, Oct. 2014.

[8] Z. Azar, Z. Q. Zhu, and G. Ombach, "Influence of electric loading and magnetic saturation on cogging torque, back-EMF and torque ripple of PM machines," *IEEE Trans. Magn.*, vol. 48, no. 10, pp. 2650-2658, Oct. 2012.